Optics Communications 283 (2010) 2438–2441

Contents lists available at ScienceDirect

Optics Communications

journal homepage: www.elsevier.com/locate/optcom

Distributed strain measurement using a tellurite glass fiber with Brillouin optical correlation-domain reflectometry

Yosuke Mizuno *, Zuyuan He, Kazuo Hotate

Department of Electrical Engineering and Information Systems, The University of Tokyo, 7-3-1 Hongo, Bunkyo-ku, Tokyo 113-8656, Japan

ARTICLE INFO

Article history:
Received 19 November 2009
Received in revised form 1 February 2010
Accepted 1 February 2010

Keywords:
Tellurite glass fiber
Brillouin scattering
Brillouin frequency shift
Distributed strain measurement
Nonlinear optics

ABSTRACT

A tellurite glass fiber with a high Brillouin gain was employed for distributed strain measurement with Brillouin optical correlation-domain reflectometry (BOCDR). First, the spatial resolution of BOCDR was evaluated using the tellurite fiber. With the high Brillouin gain of the fiber, it was confirmed clearly in the experiment that the spatial resolution is limited by the Rayleigh scattering-induced noise. Then, the dependence of the Brillouin frequency shift (BFS) on strain in the tellurite fiber was investigated, showing a negative dependence with a coefficient of -0.023 MHz/$\mu\varepsilon$. Using this tellurite fiber, the distribution of the BFS around a 1-cm strain-applied section was successfully measured with BOCDR of a nominal spatial resolution of 6 mm.

1. Introduction

Brillouin optical correlation-domain reflectometry (BOCDR) [1] can measure the distribution of strain and/or temperature along a fiber under test (FUT) from a single end. So far, 13-mm spatial resolution has been achieved [2]. Although this resolution is the best ever reported in spontaneous Brillouin scattering-based reflectometers, it was limited by the signal-to-noise (S/N) ratio in the conventional silica fiber-based Brillouin gain spectrum (BGS) measurement. It is expected that the spatial resolution can be improved by using a specialty fiber with a large Brillouin gain coefficient as the FUT to enhance the S/N ratio.

Among various specialty fibers, tellurite glass fibers [3,4] have been vigorously studied due to their high refractive index ($n = 2.03$), high nonlinearity, and broad Raman gain bandwidth, and thus far been applied to developing optical devices, such as ultra-wide-band Raman fiber amplifiers (RFAs) [5], efficient Tm^{3+}-doped tellurite fiber lasers [6], and carrier-envelope offset (CEO)-locked frequency combs [7]. In addition to these applications, they can also be used as the gain medium for Brillouin scattering. Abedin [4] investigated the properties of stimulated Brillouin scattering (SBS) and the performance of slow light generation in an Er^{3+}-doped tellurite fiber, and showed that a tellurite fiber has a large Brillouin gain coefficient ($g_B \sim 1.7 \times 10^{-10}$ m/W) and is suitable for slow light generation.

In this paper, a tellurite fiber is employed in BOCDR to realize high-spatial-resolution distributed strain sensing. Although the background loss ($\sim$0.02 dB/m at 1550 nm) of the tellurite fibers is much higher than that of silica fibers ($\sim$0.0005 dB/m), making use of their high Brillouin gain, we believe tellurite fibers can be applied to developing short-range but high-spatial-resolution Brillouin sensors. First, the spatial resolution of BOCDR using the tellurite fiber is evaluated. With the high Brillouin gain of the fiber, it is confirmed clearly in the experiment that the spatial resolution is limited by the Rayleigh scattering-related noise. Next, the strain-dependence of the Brillouin frequency shift (BFS) in a tellurite fiber is investigated. It is found that, with increasing strain, the BFS in the tellurite fiber shifts toward lower frequency with a coefficient of -0.023 MHz/$\mu\varepsilon$. This negative dependence seems to be caused by the negative strain-dependence of the Young's modulus of the tellurite fiber. Then, a distributed strain measurement is performed by using this tellurite fiber as the FUT in BOCDR with a nominal spatial resolution of 6 mm, which is the inherent limitation as described later.

2. Principles

Brillouin scattering occurs when light is Bragg-reflected by the refractive index modulations produced by acoustic phonons. The backscattered light (Stokes light) suffers a Doppler shift called BFS, which depends on tensile strain applied to the optical fiber. For example, in a standard silica single-mode optical fiber (SMF), the BFS of about 11 GHz slightly varies to higher frequency in proportion to the applied strain with a coefficient of +0.058 MHz/$\mu\varepsilon$

* Corresponding author. Tel.: +81 3 5841 6768; fax: +81 3 5841 6025.
E-mail addresses: ymizuno@sagnac.t.u-tokyo.ac.jp (Y. Mizuno), ka@sagnac.t.u-tokyo.ac.jp, hotate@sagnac.t.u-tokyo.ac.jp (K. Hotate).

0030-4018/$ - see front matter © 2010 Elsevier B.V. All rights reserved.
doi:10.1016/j.optcom.2010.02.002

[8]. Hence, the BFS can provide the information on the strain magnitude in the fiber.

BOCDR is based on spontaneous Brillouin scattering. As described in [1], its basic principle is to generate a correlation peak within the FUT by applying the same frequency modulation to the pump and the reference light. The experimental setup is the same as that reported previously [9], where a polarization scrambler was inserted in the reference path to suppress the polarization-dependent fluctuations of the BGS. The measurement range d_m (distance between the correlation peaks) is given by

$$d_m = \frac{c}{2nf_m}, \tag{1}$$

where c is the velocity of light in vacuum, n the refractive index, and f_m the modulation frequency of the light source. The following expression of the spatial resolution Δz was derived for BOCDA [10,11], but it also holds well for BOCDR according to our previous experimental results [1,2,9]:

$$\Delta z = \frac{c\Delta\nu_B}{2\pi n f_m \Delta f}, \tag{2}$$

where $\Delta\nu_B$ is the Brillouin gain bandwidth in optical fibers, and Δf is the modulation amplitude of the light source. Here, it is known that f_m higher than $\Delta\nu_B$ does not contribute to the enhancement of Δz in Eq. (2) [10]. In addition, Δf must be lower than a half of the BFS of the FUT because of the behavior of Rayleigh scattering-related noise in BOCDR as described schematically in [1]. Therefore, under the condition of $f_m = \Delta\nu_B$, the limitation of the spatial resolution Δz_{min} is given, by the BFS, as

$$\Delta z_{min} = \frac{c}{\pi n \mathrm{BFS}} \tag{3}$$

In Table 1, n, BFS, and Δz_{min} of silica, bismuth oxide [12], As_2Se_3 chalcogenide [13], and tellurite fibers are summarized. About 6-mm spatial resolution is expected by using a tellurite fiber.

3. Experiments

First, we evaluated experimentally the spatial resolution of BOCDR using the tellurite fiber. The structure of the FUT is depicted in Fig. 1. Since it is difficult to directly splice a tellurite fiber (5 m) to an SMF with a good mode matching, a dispersion-compensation fiber (DCF) (30 cm) was inserted between them. One end of the tellurite fiber was connected to the DCF with a tilted V-groove connection [14], and the other end was bent to suppress the Fresnel reflection. The light-source modulation frequency f_m was set to 7.8028 MHz to place a correlation peak within the tellurite fiber.

Fig. 2 shows the whole spectra of the electrical output of the BOCDR system when Δf was increased from 0.1 to 4.0 GHz. Due to the large Brillouin gain coefficient of the tellurite fiber, along with its strong Rayleigh scattering, the evolution of the spectra was observed much more clearly than that in our previous experiment [1]. As Δf became larger, the spectrum of the Brillouin-scattered light broadened in both directions for $2\Delta f$ around the BGS peak at about 8 GHz. The BGS peak frequency gives the BFS at a specific position in the FUT selected by the light-source frequency modulation. This is the mechanism of the distributed measurement of BOCDR [1]. In Fig. 2, a large amount of noise spreading from 0 Hz to $2\Delta f$ is also clearly shown, which is induced by the Rayleigh scattering. When Δf was 4.0 GHz, the noise began to overlap the BGS peak. This result confirms experimentally that the limitation of Δf is a half of the BFS of the fiber, and thus the spatial resolution must be larger than the value given in Eq. (3).

Next, the strain-dependence of the BFS in the tellurite fiber was investigated using the same FUT. Since the tellurite fiber was short, the measurement was conducted using BOCDR to place the measurement window (the correlation peak) within the tellurite fiber to remove the effects of other fibers. Δf and f_m were set to 1 GHz and 7.8028 MHz, respectively, which correspond to the measurement range d_m of 9.47 m and the spatial resolution Δz of about 3 cm according to Eqs. (1) and (2). As shown in Fig. 3, $\Delta\nu_B$ was 10 MHz, which is much narrower than those of more than 23 MHz reported so far [4,15] probably due to the high-gain condition and the difference in glass purity. In the tellurite fiber, different strains were applied to a 40-cm section (5.7–6.1 m from the

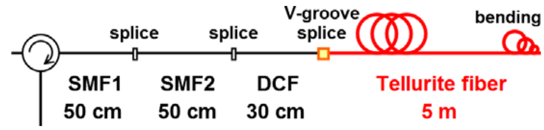

Fig. 1. Structure of the FUT.

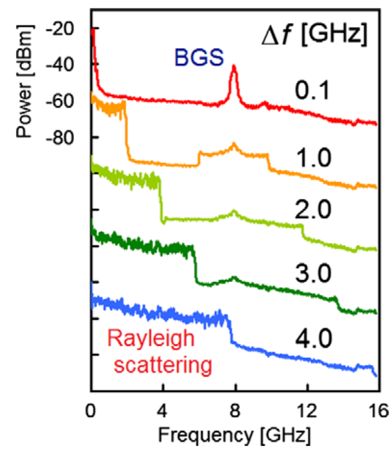

Fig. 2. Electrical spectra when the modulation amplitude Δf was increased from 0.1 to 4.0 GHz. Each spectrum is shifted by 35 dB. The values on the ordinate are valid only for Δf = 0.1 GHz.

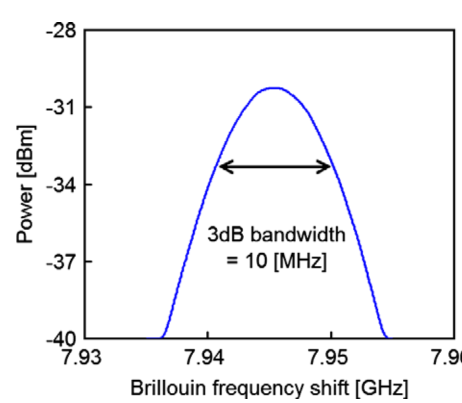

Fig. 3. Measured BGS from 5-m tellurite fiber with no strain applied.

Table 1
n, BFS, and Δz_{min} of silica, bismuth-oxide [12], As_2Se_3 chalcogenide [13], and tellurite fibers.

Fiber	n	BFS (GHz)	Δz_{min} (mm)
Silica	1.46	10.86	6.0
Bismuth oxide	2.22	8.83	4.9
Chalcogenide	2.8	7.97	4.3
Tellurite	2.03	7.95	5.9

circulator) fixed on a translation stage using epoxy glue. The position of the correlation peak was set to the middle of the strain-applied section, and the sampling rate of the BGS measurement was about 2 Hz including 10-times averaging.

The strain-dependence of the BGS in the tellurite fiber is shown in Fig. 4a. With increasing the applied strain, the BGS shifted toward lower frequency. From these spectra, we can plot the strain-dependence of the BFS as shown in Fig. 4b. The error bars are ±2.5 MHz, corresponding to the BFS fluctuations when strain was fixed. The slope of the straight-line approximation was calculated to be −0.023 MHz/με. It is notable that the sign of the strain-dependence is opposite to that of a silica SMF (+0.058 MHz/με [8]).

In general, the strain coefficient of the normalized BFS in optical fibers is given by:

$$\frac{1}{\nu_B}\frac{\partial \nu_B}{\partial \varepsilon} = \frac{1}{n}\frac{\partial n}{\partial \varepsilon} + \frac{1}{2E}\frac{\partial E}{\partial \varepsilon} - \frac{1}{2\rho}\frac{\partial \rho}{\partial \varepsilon}, \tag{4}$$

where E is the Young's modulus, and ρ the density. The values of each term have been determined as −0.23, 2.88, and 0.36 by Horiguchi et al. [8] for silica fibers with $n = 1.46$. Since the BFS is about 10.86 GHz in SMFs, the strain coefficient is calculated to be +0.033 MHz/με, which roughly matches the measured value (+0.058 MHz/με). In order to estimate the case of tellurite fibers with $n = 2.03$, we make two assumptions as follows: (i) the first term is −0.445 ($= -0.23 \times 2.03^2/1.46^2$) because it is proportional to the square of n [8], and (ii) the third term is 0.16 ($= 0.36 \times 2.2/5.1$) because ρ of silica crystals is 2.2 g/cm^3, while that of tellurite crystals is 5.1 g/cm^3 [16]. Using the measured strain coefficient (−0.023 MHz/με), the second term can be calculated back to be −2.61. This negative dependence of the Young's modulus on strain has been observed also in soda glass fibers (silica + Na_2O + CaO) by Mallinder et al. [17], with a second term of −2.555. Thus, we presume that the negative strain-dependence of the BFS is due to the negative dependence of the Young's modulus on strain in the tellurite fiber.

Finally, this tellurite fiber was employed as the FUT in distributed strain measurement by BOCDR to improve the S/N ratio and thus to achieve the inherent limitation of the spatial resolution given by Eq. (3). The modulation frequency f_m was set to 9.972599–9.975924 MHz ($f_m \leqslant \Delta\nu_B$ of the tellurite fiber), which corresponds

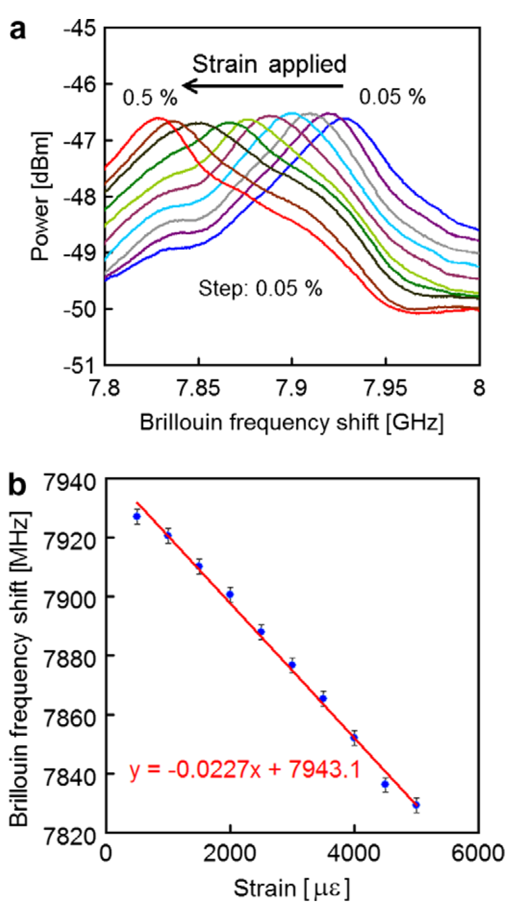

Fig. 4. (a) Strain-dependence of the BGS in the tellurite fiber and (b) that of the BFS.

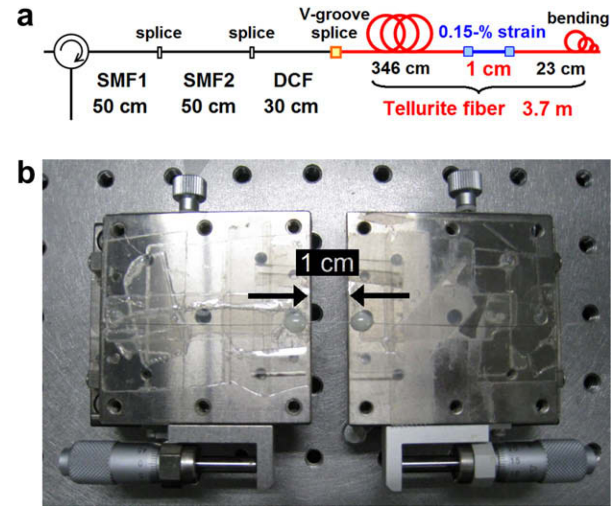

Fig. 5. (a) Structure of the FUT for a distributed measurement and (b) photo of the strain-applied section.

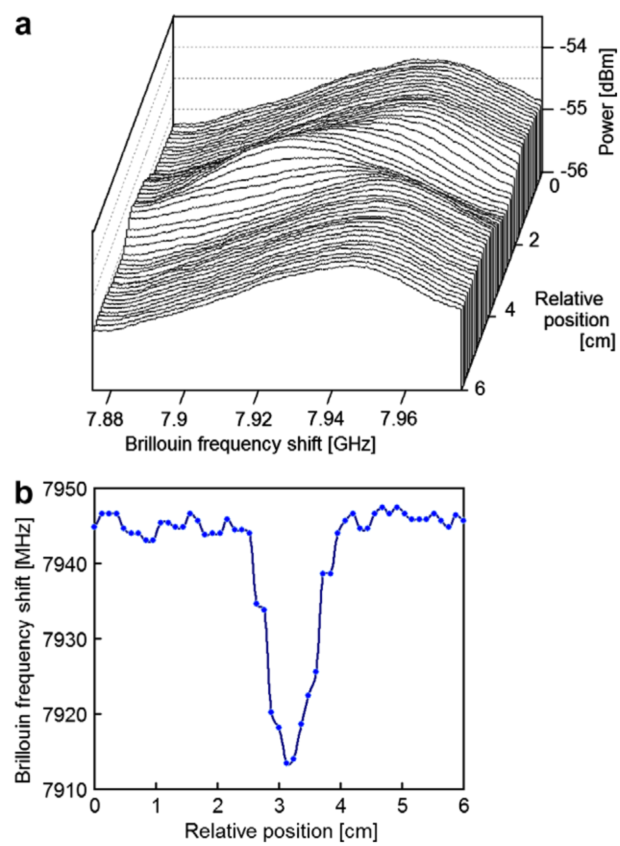

Fig. 6. (a) Measured distribution of the BGS along the FUT and (b) that of the BFS.

to a measurement range d_m of 7.4 m according to Eq. (1). The amplitude of the frequency modulation Δf was 3.94 GHz ($\Delta f \leqslant$ BFS/2), and the nominal spatial resolution Δz was calculated to be about 6 mm from Eqs. (2) and (3). The structure of the FUT is shown in Fig. 5a and b. The length of the tellurite fiber was 3.7 m, and 0.15% strain was applied to a 1-cm section. Other conditions concerning the FUT were the same as those for the preceding measurement. Polarization scrambling was employed, and the sampling rate of the measurement for a single position was 10 Hz including 5-times averaging. The measurement was performed at 50 points sequentially for 5 s.

Fig. 6a shows the measured distribution of the BGS along the FUT. The BGS at the strain-applied section was recognized with much higher S/N ratio than that in our previous experiment with an SMF as the FUT [2]. Fig. 6b shows the distribution of the BFS. The 1-cm strain-applied section was detected with a nominal spatial resolution of 6 mm, which is the inherent limitation given by Eq. (3). The gradual variation of the BFS seems to have come from the strain distribution inside the epoxy glue. The change of the BFS was about −34 MHz, which corresponds to 0.148% strain. This value is in good agreement with the applied strain of 0.15%. The accuracy of the measurement at a single position was about ±2.5 MHz, which corresponds to a strain accuracy of ±0.01% (±100 $\mu\varepsilon$ in this experiment.

4. Conclusions

We employed a tellurite fiber as the FUT in BOCDR to realize a short-range but high-spatial-resolution distributed strain measurement. The spatial resolution of BOCDR was evaluated experimentally using the tellurite fiber. Thanks to the high Brillouin gain of the fiber, the behavior of Rayleigh scattering-induced noise in BOCDR was observed clearly. This experiment confirmed that the modulation amplitude Δf of the light source is inherently limited to below a half of the BFS of the fiber, and thus the spatial resolution is correspondingly limited. The investigation on the dependence of the BFS on strain in the tellurite fiber shows that the BFS in this kind of fiber shifted toward lower frequency with increasing strain, and its coefficient was found to be −0.023 MHz/$\mu\varepsilon$. This negative dependence seems to originate from the negative dependence of the Young's modulus of the tellurite fiber on strain. A distributed strain measurement with BOCDR was demonstrated using the tellurite fiber. With the high Brillouin gain of the tellurite fiber and thus the enhanced S/N ratio in BGS measurement, a 1-cm strain-applied section was successfully detected with 6-mm nominal spatial resolution, which is the inherent limitation of the fiber. This is the first demonstration of a millimeter-order spatial resolution among one-end-access strain-sensing reflectometers. We expect the BOCDR system to be useful not only in strain monitoring of civil structures but also in the investigation of internal structures of optical components because of its high-resolution measurability.

Acknowledgements

The authors are grateful to Dr. Atsushi Mori of NTT Photonics Laboratories, Japan, for providing the tellurite glass fiber sample. One of the authors (Y.M.) thanks the Japan Society for the Promotion of Science (JSPS) Research Fellowships for Young Scientists. This work was supported by the Grant-in-Aid for Scientific Research (S) and the Global Center of Excellence (G-COE) Program from the Ministry of Education, Culture, Sports, Science and Technology (MEXT), Japan.

References

[1] Y. Mizuno, W. Zou, Z. He, K. Hotate, Opt. Express 16 (2008) 12148.
[2] Y. Mizuno, Z. He, K. Hotate, IEEE Photon. Technol. Lett. 21 (2009) 474.
[3] J.S. Wang, E.M. Vogel, E. Snitzer, Opt. Mater. 3 (1994) 187.
[4] K.S. Abedin, Opt. Express 14 (2006) 11766.
[5] A. Mori, H. Masuda, K. Shikano, M. Shimizu, J. Lightwave Technol. 21 (2003) 1300.
[6] B. Richards, Y. Tsang, D. Binks, J. Lousteau, A. Jha, Opt. Lett. 33 (2008) 402.
[7] A. Ishizawa, T. Nishikawa, S. Aozasa, A. Mori, O. Tadanaga, M. Asobe, H. Nakano, Opt. Express 16 (2008) 4706.
[8] T. Horiguchi, T. Kurashima, M. Tateda, IEEE Photon. Technol. Lett. 1 (1989) 107.
[9] Y. Mizuno, Z. He, K. Hotate, Appl. Phys. Express 2 (2009) 062403.
[10] K. Hotate, T. Hasegawa, IEICE Trans. Electron. E83-C (2000) 405.
[11] K.Y. Song, Z. He, K. Hotate, Opt. Lett. 31 (2006) 2526.
[12] J.H. Lee, T. Tanemura, K. Kikuchi, T. Nagashima, T. Hasegawa, S. Ohara, N. Sugimoto, Opt. Lett. 30 (2005) 1698.
[13] K.Y. Song, K.S. Abedin, K. Hotate, M.G. Herraez, L. Thevenaz, Opt. Express 14 (2006) 25.
[14] M. Yamada, A. Mori, K. Kobayashi, H. Ono, T. Kanamori, K. Oikawa, Y. Nishida, Y. Ohishi, IEEE Photon. Technol. Lett. 10 (1998) 1244.
[15] K.Y. Song, K.S. Abedin, K. Hotate, Opt. Express 16 (2008) 225.
[16] A. El-Adawy, R. El-Mallawany, J. Mater. Sci. Lett. 15 (1996) 2065.
[17] F.P. Mallinder, B.A. Proctor, Phys. Chem. Glass 5 (1964) 91.